

Structural and Optical Studies of the Topochemical Polymerization Mechanism of the Bis(*p*-toluenesulfonate) of 2,4-Hexadiyne-1,6-diol

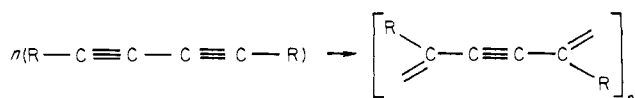
P. A. Albouy,* P. Keller,[†] and J. P. Pouget

Contribution from the Laboratoire de Physique des Solides, Associé au C.N.R.S., Université de Paris Sud—Bâtiment 510, 91405 Orsay, France. Received February 3, 1982

Abstract: The mechanism of thermal polymerization in PTS (the bis(*p*-toluenesulfonate) of 2,4-hexadiyne-1,6-diol) single crystals has been investigated by X-ray diffraction and visible spectroscopy. It has been shown that the reaction proceeds homogeneously with polymer chains growing at random in the crystal. Their average length has been directly measured by X-ray diffuse scattering as a function of polymer conversion in the induction period. An average polymer chain length of about 100 Å (20 units) has been determined at the beginning of the induction period and gradually increases to about 200 Å (40 units) at the end of this period. Very similar results have been obtained by an elastic analysis of the behavior of the lattice parameter in the chain direction. In the autocatalytic period, long chains (>700 Å) abruptly appear. The absorption spectrum (500–700 nm) of polymer chains has been followed as a function of conversion, and qualitative information concerning the chain length distribution function has been drawn from its behavior.

I. Introduction

Some diacetylenes of formula $R-C\equiv C-C\equiv C-R'$, where R and R' are two side groups, have the remarkable property to undergo a progressive topochemical polymerization where monomer single crystals are transformed into nearly defect-free polymer single crystals.¹ The reaction can be initiated either thermally by annealing or photochemically by exposure to ionizing radiation. Among diacetylenes, the bis(*p*-toluenesulfonate) of 2,4-hexadiyne-1,6-diol (PTS) where $R = R' = -CH_2-O-SO_2-Ph-CH_3$ has been extensively studied and is considered as a model compound. The reaction process can be described² as a 1,4 addition of adjacent monomer units in a particular crystallographic direction according to



During the solid-state transformation, the tilt of the four central carbon atoms with respect to the polymerization direction decreases from about 45° in the pure monomer to about 14° in the pure polymer, while side groups R keep nearly the same orientation.³ It has been shown that side groups play a crucial role by fixing the packing geometry of the monomer crystal and by their ability to smoothen the stresses caused by the polymerization process.¹

Two mechanisms have been proposed for this reaction: a heterogeneous mechanism with nucleation or a homogeneous process in the form of a solid solution.¹ Earlier X-ray studies have shown directly that the second process is realized in PTS.⁴ Polymer chains grow independently from one another and a partly polymerized crystal may thus be considered as a solid solution of polymer chains all extended along a common crystallographic axis (the monoclinic axis b for PTS) in a monomer matrix. Moreover, both monomer and polymer locally adopt the same periodicity along the b direction with a value intermediate between that of the pure monomer (5.18 Å) and that of the fully polymerized crystal (4.91 Å). The homogeneity of the reaction has been recently questioned by a neutron scattering study on partly polymerized crystals.⁵

Two main features characterize the thermal polymerization kinetics:⁶ an induction period up to about 15% polymer conversion during which the reaction proceeds at a slow rate, followed by an autocatalytic period during which the reaction dramatically speeds up. Both periods follow a first-order kinetics and have

nearly the same activation energy of about 22 kcal/mol.⁶ The reaction rate increases by 2 orders of magnitude in the autocatalytic period.⁶ It seems that the activation energy is mainly related to the formation of activated species.⁷ The reaction-speed acceleration is now believed⁸ to correspond to a sudden increase of the length of newly formed chains. As already stated, first polymer chains have the monomer periodicity and experience thus an elongation of about 5% with respect to the polymer natural periodicity. It results in a cost in elastic energy which hinders a further growth of polymer chains. As the reaction proceeds, the monomer matrix becomes more and more stressed by the growing amount of polymer so that the tension on the polymer chains is gradually released. Above about 15% conversion, these elastic stresses have relaxed enough to allow a massive growth of polymer. In the autocatalytic period an average polymer chain length of about 5 μm has been estimated by electronic microscopy.⁹

These elastic considerations are of primary importance for a macroscopic understanding of the solid-state polymerization process. They have been used in a kinetics model worked out by Baughman.¹⁰ However, a microscopic apprehension of the reaction mechanism requires the knowledge of chain lengths and their distribution function as a function of the polymer content. If we bear in mind the magnitude of the length of the first polymer chains already estimated by several authors (around 100 Å^{4,8}), the X-ray diffuse scattering method appears to be a well-adapted technique for the study of the induction period. Moreover, complementary information on the chain length distribution function can be obtained from spectroscopic measurements via the electronic structure of short polymer chains.

This paper has been divided as follows: experimental conditions are given in part II, the X-ray study is presented in part III, and the spectroscopic study is given in part IV. Several conclusions

(1) Wegner, G. "Chemistry and Physics of One-Dimensional Metals"; H. J. Keller: New York, 1976; p 297 ff. Wegner, G. "Molecular Metals"; W. H. Hatfield: New York, 1979; p 209 ff.

(2) Wegner, G. *Makromol. Chem.* **1972**, *154*, 35.

(3) Enkelmann, V.; Leyrer, R. J.; Wegner, G. *Makromol. Chem.* **1979**, *180*, 1787. Almè, J. P.; Lefevre, J.; Bertault, M.; Schott, M.; Williams, J. O. *J. Phys.* **1982**, *43*, 307.

(4) Robln, P.; Pouget, J. P.; Comès, R.; Moradpour, A. *J. Phys.* **1980**, *41*, 415.

(5) Grimm, H.; Axe, J. D.; Kröhnke, C. *Phys. Rev. B* **1982**, *25*, 1709.

(6) McGhlie, A. S.; Kalyanaraman, P. S.; Garito, A. F. *J. Polym. Sci., Polym. Lett. Ed.* **1978**, *16*, 335.

(7) Chance, R. R.; Patel, G. N. *J. Polym. Sci., Polym. Phys. Ed.* **1978**, *16*, 859.

(8) Chance, R. R.; Sowa, J. M. *J. Am. Chem. Soc.* **1977**, *99*, 6703.

(9) Mondong, R.; Bässler, H. *Chem. Phys. Lett.* **1981**, *78*, 371.

(10) Baughman, R. H. *J. Chem. Phys.* **1978**, *68*, 3110.

[†] Laboratoire de Synthèse Asymétrique, Université de Paris Sud—Bâtiment 420, 91405 Orsay, France.

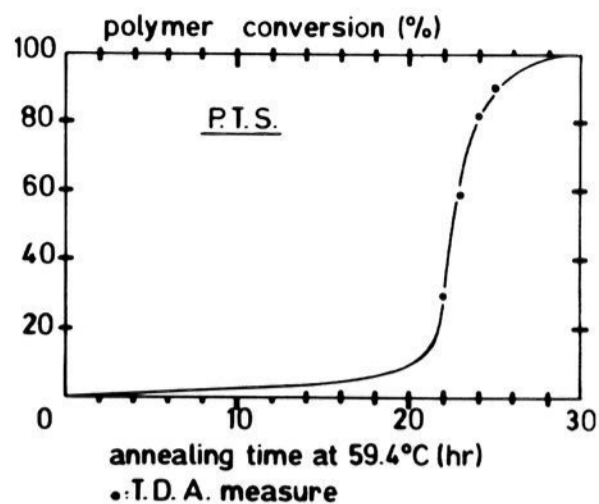


Figure 1. Conversion curve (polymer content vs. annealing time). The curve which has been obtained at 60 °C by differential scanning calorimetry by Bertault¹² has been adjusted by homothetic transposition to our annealing temperature, 59.4 °C, by points (full dots) determined by thermal differential analysis.

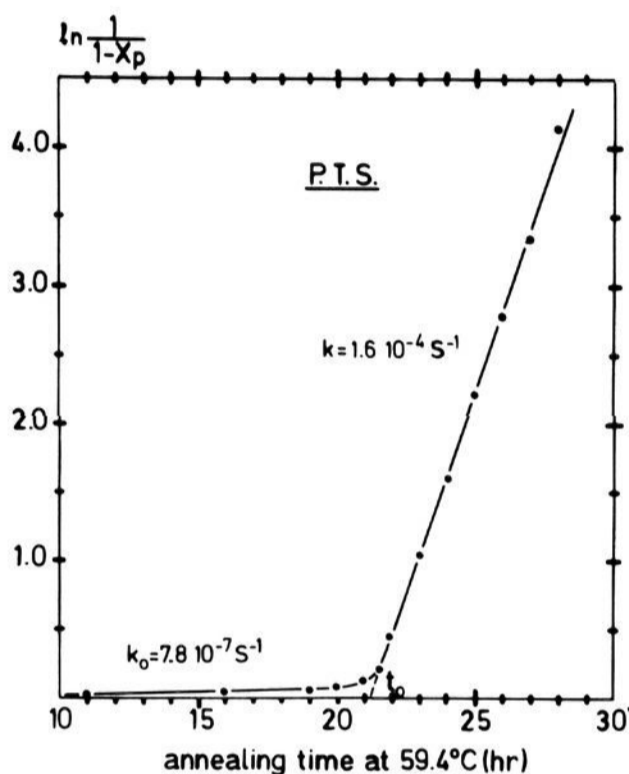


Figure 2. $\ln [1/(1 - x_p)]$ as a function of the annealing time at 59.4 °C. $t_0 = 21.25$ h represents the conventional transition time between induction and autocatalytic periods. k_0 and k , respectively, represent the first-order rate constants in induction and autocatalytic regimes.

on the solid-state polymerization mechanism of PTS will be drawn in part IV.

II. Experimental Section

(a) Sample Preparation. Crystals of PTS monomer were grown from acetone solution by slow evaporation at about 0 °C according to well-known procedures.¹¹ Single crystals used for X-ray study had an optimum size of about $0.5 \times 1 \times 3$ mm³. A different crystal has been used for each measurement.

Polymerization was performed by thermal annealing at 59.4 °C. The conversion curve (Figure 1) has been obtained by adjusting a curve precisely determined by differential scanning calorimetry (DSC) at 60 °C¹² with several points obtained by thermic differential analysis (TDA) with our own annealed crystals. As both periods follow a first-order kinetics,⁶ that is $dx_p/dt = k(1 - x_p)$, x_p being the polymer content, we have plotted $\ln [1/(1 - x_p)]$ as a function of the annealing time (Figure 2). The two regimes of polymerization clearly appear: (i) induction period for $t < t_0 = 21.25$ h, that is, $x_p < 15\%$; we find a first-order rate constant $k_0 = 4.8 \times 10^{-7} \text{ s}^{-1}$; (ii) autocatalytic period for $t > t_0$; the first-order rate constant has the value $k = 1.6 \times 10^{-4} \text{ s}^{-1}$. The speed increase in the autocatalytic period $k/k_0 = 210$ agrees with previous reports.⁶

(11) Wegner, G. *Makromol. Chem.* **1971**, *145*, 85.

(12) Bertault, M., private communication. As for the use of DSC, see, for instance: Chance, R. R.; Patel, G. N.; Turi, E. A.; Khanna, Y. P. *J. Am. Chem. Soc.* **1978**, *100*, 1307.

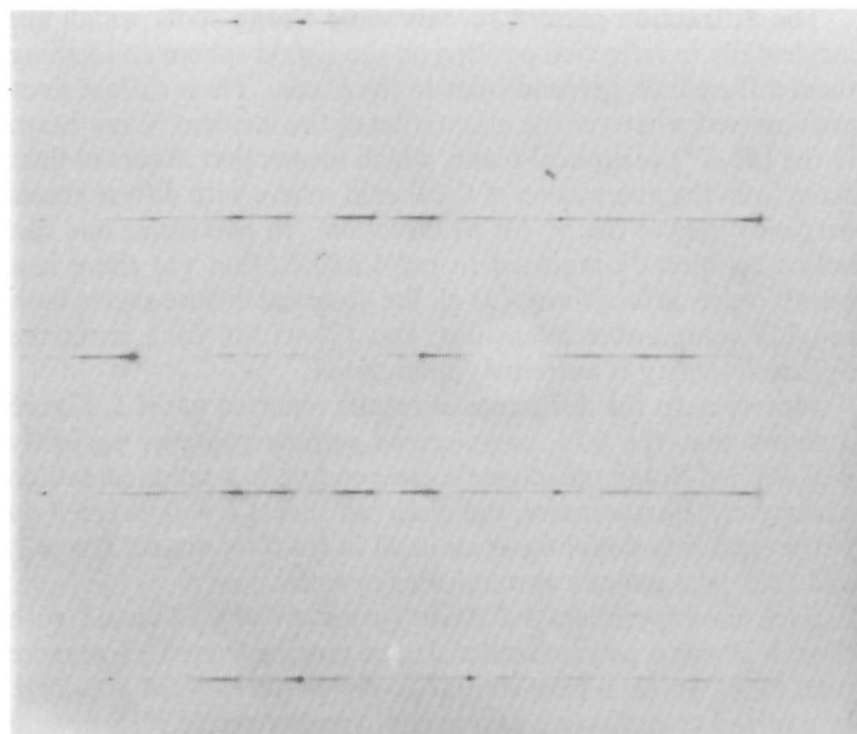


Figure 3. X-ray pattern of partially polymerized crystal ($x_p = 60\%$) taken with the synchrotron radiation of LURE (exposure time: 5 min). The chain axis b is vertical.

(b) X-ray Apparatus. The X-ray study was performed with monochromatic Cu $K\alpha$ radiation from reflection on a doubly curved pyrolytic graphite monochromator. Diffuse scattering X-ray patterns were obtained with the fixed film, fixed crystal method known as the "monochromatic Laue technique". As PTS crystals rapidly polymerize under x-ray irradiation at room temperature, the experiment has been carried out with crystals cooled at 25 K with a CTI "cryodyne Cryocooler". As already pointed out by several authors, samples irradiated by UV¹³ or X-ray⁴ at low temperature begin to polymerize markedly when warmed up above around 90 K. In the present study we have never been able to detect any change in the diffuse scattering at 25 K for previously annealed samples whatever the exposure time, showing that the polymerization is completely frozen at such a low temperature.

The collimation of the X-ray apparatus was chosen with the compromise to have a good resolution with enough intensity to detect the diffuse scattering. The resolution was determined either by the width of weak Bragg reflections coming from the $\lambda/2$ contamination or by the width of Debye-Scherrer rings of Al powder obtained under the same conditions. Both results were in agreement and gave a resolution: $\delta b^*_{\text{res}} = 0.014 \text{ \AA}^{-1}$ (half-width at half-maximum (hwhm)). (The convention $\vec{b} \cdot \vec{b}^* = 2\pi$ for the reciprocal lattice has been used throughout this study.) Higher-resolution X-ray patterns ($\delta b^*_{\text{res}} = 0.006 \text{ \AA}^{-1}$) have also been obtained at the station D16 of the synchrotron radiation of LURE (Orsay).

X-ray patterns have been read with a Joyce-Loeble microdensitometer. Results presented in this paper correspond to an average of several scans.

The determination of the crystallographic parameter b was made at room temperature with a conventional precession camera mounted on a high-intensity rotating anode source equipped with a 100- μm focus. Crystals were optically oriented on the precession camera.

(c) Spectroscopy Apparatus. Transmission spectra (500–700 nm) were recorded with a Cary 219 spectrometer. To obtain these spectra from the beginning to the end of the polymerization, we used very thin crystals. For this purpose we have adapted a technique already described by Bloor.¹⁴ A drop of a dilute solution of PTS monomer in acetone was put on a glass plate. After evaporation small crystals (about $30 \times 15 \times 3 \mu\text{m}^3$ in size) were formed. The plate was then set in a heating Mettler stage and put in the spectrometer. The polymerization was thus performed "in situ" at a temperature of 75 °C. Three minutes was needed to record a spectrum.

III. X-ray Study of the Polymerization Mechanism of PTS

(a) Basic Experimental Facts. Figure 3 shows a fixed-film, fixed-crystal diffraction pattern of a partially polymerized crystal obtained with the synchrotron radiation of LURE (conversion: 60%). The b axis has been set as indicated and is perpendicular to the X-ray beam. The position of the two other axes \vec{a} and \vec{c} is not fixed in any particular way.

(13) Hersel, W.; Sixl, H.; Wegner, G. *Chem. Phys. Lett.* **1980**, *73*, 288.

(14) Bloor, D.; Williams, R. L.; Ando, D. J. *Chem. Phys. Lett.* **1981**, *78*, 67.

The diffraction pattern reveals some Bragg spots which are incidentally in reflection position on the Ewald sphere and joining them diffuse lines perpendicular to the b axis. These diffuse lines are observed whatever the orientation of the incident X-ray beam in the (\bar{a}^* , \bar{c}^*) reciprocal plane, which means that observed lines come from the intersection of the Ewald sphere with diffuse sheets perpendicular to the b^* (or b) direction. In particular one can notice, as already reported in ref 4 and 5, that (1) there is a zeroth-order diffuse sheet, (2) all the observed diffuse sheets have roughly comparable intensities, and (3) within each sheet the diffuse intensity is extremely modulated.

Moreover, at the difference of results reported in ref 5, Figure 3 shows that the 60% polymerized sample presents perfectly well-defined Bragg reflections corresponding to a unique b lattice parameter. Furthermore, the observed sheets $k = 0, \pm 1, \pm 2$ do not present any doubling as claimed in ref 5 for sheets $k = \pm 3$, and they pass exactly through Bragg reflections.

Such an experiment has been systematically repeated with crystals having a polymerization degree ranging from 0.3% to more than 99%. In each case similar X-ray patterns were obtained. In a mixed crystal, such as a partially polymerized PTS crystal made out of polymer and monomer units, the idea of average lattice can be introduced. This lattice gives rise to Bragg spots, the intensity of which depends on an average structure factor. The intensity scattered outside the Bragg reflections (diffuse diffusion) reflects the local differences between the real crystal and the average lattice.¹⁵ For the sake of simplicity, we can first look at a poorly polymerized crystal. In such a case, the average lattice and the monomer lattice are practically the same. The difference between the real and average lattices is thus made up of chains corresponding to the polymer chains but having a structure factor equal to the difference of the structure factors of the polymer and monomer. The reciprocal lattice of an isolated chain of length \bar{l} and parameter b is made up of equidistant and parallel sheets perpendicular to the chain axis with a spacing $2\pi/b$. The width of the sheets is related to the chain length by the Scherrer formula which will be given below. In the case of a poorly polymerized crystal the intensities diffracted by the isolated chains just add. When the polymer concentration increases, the average lattice cannot be approximated by the monomer lattice anymore and polymer and monomer have to be treated on an equal footing. In any case, the observed sheets are the direct consequence of the anisotropy of the reaction. The very important point to emphasize is that the diffuse lines always pass through the Bragg reflections. This is the direct proof that polymer chains have locally the same parameter b as the average lattice during the whole reaction. It means that there is only one lattice periodicity between polymer and monomer units along the b direction.

Let us first discuss the change of the b lattice parameter as a function of the polymer content.

(b) Variation of b Parameter. Such a study has already been published,^{3,4} but it seemed interesting to determine a perhaps more precise curve that will be quantitatively analyzed below. The curve is displayed in two parts in Figure 4. The upper one (A) shows the parameter b at room temperature as a function of the annealing time. It presents a characteristic sharp decrease in the auto-catalytic period. This curve is to compare with Figure 1, giving the polymer content as a function of the annealing time. The lower curve (B) gives the relative variation of the b parameter as a function of the polymer content. b_m and b_p respectively represent the parameter of the monomer and of the polymer ($b_m = 5.165$ Å and $b_p = 4.904$ Å with our determinations). We have tried to go a little further in the analysis of these results by using the bases of an elastic model developed by Baughman.¹⁰ In a mixed crystal of polymer content x_p , the elastic energy can be written as

$$U_{\text{elastic}} = \frac{1}{2}x_p E_p (b - b_p)^2 + \frac{1}{2}(1 - x_p) E_m (b - b_m)^2$$

E_m and E_p being respectively the elastic moduli of the monomer

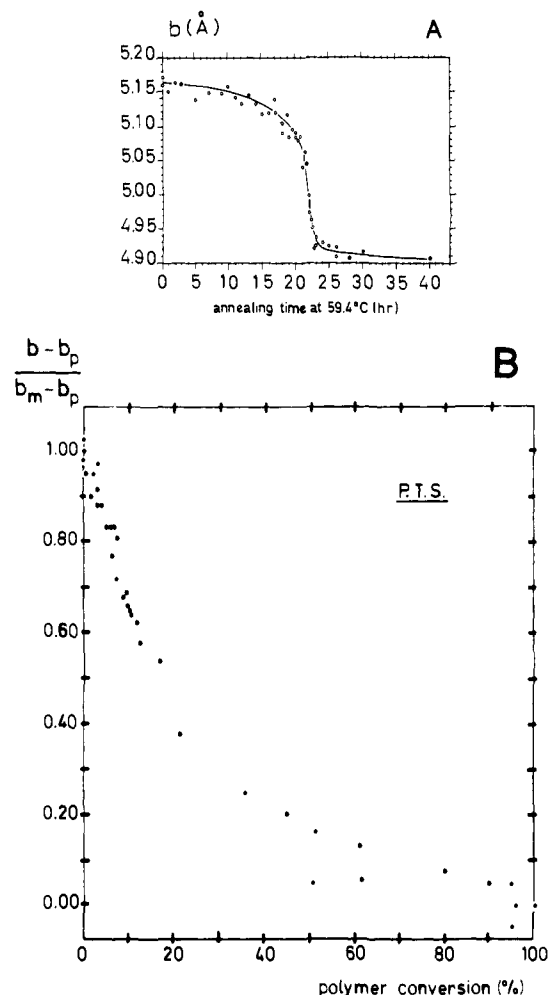


Figure 4. (A) Monoclinic parameter, b , of the average lattice of PTS as a function of the annealing time at 59.4 °C. (B) Relative change of the b parameter, $(b - b_p)/(b_m - b_p)$ as a function of the polymer content, x_p .

and of the polymer in the b direction. The crystal thus adopts the b parameter which minimizes U_{elastic} ; hence

$$\frac{b - b_m}{b_m - b_p} = \frac{1}{1 + \frac{x_p E_p}{1 - x_p E_m}} \quad (1)$$

One can deduce the ratio E_p/E_m from this relation. This ratio plays a crucial role in the kinetics model of Baughman.¹⁰ For our purpose, a more convenient quantity is the ratio E_p/E_p^∞ where E_p^∞ is the elastic modulus of the pure polymer crystal. E_m , being due to van der Waals interactions between monomer units, is not expected to change substantially during polymerization. So one assumes that

$$\frac{E_p}{E_p^\infty} = \frac{E_p/E_m}{(E_p/E_m)(x_p \rightarrow 1)}$$

This quantity has been plotted in Figure 5. It is worth noting that E_p reaches the value E_p^∞ when $x_p > 15\%$. According to Rosen and Friedman,¹⁶ the ratio E_p/E_p^∞ is given by

$$\frac{E_p}{E_p^\infty} = 1 - \frac{\tanh A}{A} \quad (2)$$

where

$$A = \frac{2G_m}{E_p^\infty} \left(\frac{\bar{l}}{r} \right)^2 \frac{x_p^{1/2}}{1 - x_p^{1/2}} \quad (3)$$

(15) Guinier, A. "Théorie et Technique de la Radiocristallographie"; Dunod: Paris, 1956.

(16) Rosen, B. W.; Friedman, E. "Wisker Technology"; Wile-Interscience: New York, 1970; pp 197-224.

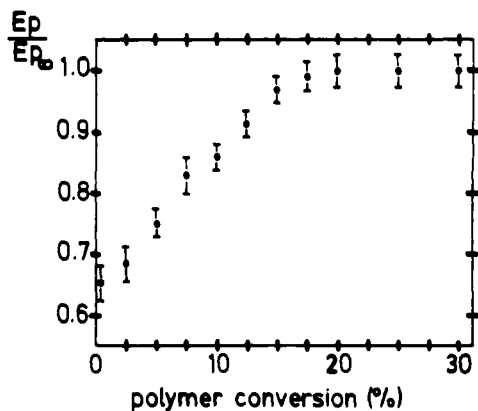


Figure 5. Ratio of elastic moduli of polymer in partly polymerized crystal E_p and fully polymerized crystal E_p^0 as a function of polymer content, x_p .

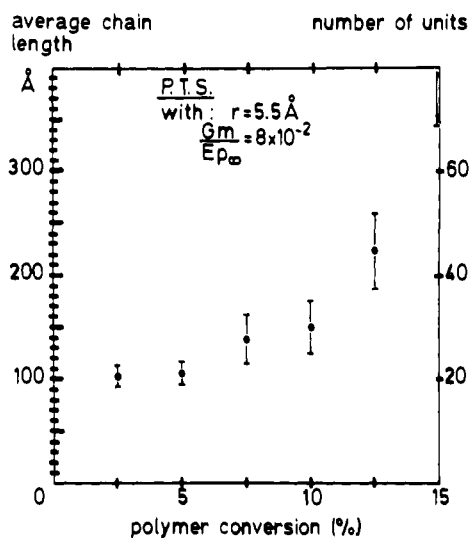


Figure 6. Average chain length, \bar{l} , as a function of polymer content, x_p , deduced from the elastic analysis of the variation of the b parameter.

\bar{l} being the average length of polymer chains, G_m the shear modulus of the monomer, and r the radius of the chain. Since there are two chains per unit cell, the "lateral spreading" of one chain is $ac \sin \beta/2$ which corresponds to an "effective radius" $r = (ac \sin \beta/2\pi)^{1/2} \approx 5.5 \text{ \AA}$. Baughman estimates that $G_m/E_p^0 \sim 8 \times 10^{-2}$.

The average length thus deduced is plotted in Figure 6. Of course, this quantity must be taken as a very rough estimation. However, it is surprising to see how correctly the value found at the beginning of the reaction ($\sim 100 \text{ \AA}$) agrees with estimated values^{4,8} and with the results of diffuse scattering measurements (see part III-c). After 15% conversion, that is, at the beginning of the autocatalytic period, E_p/E_p^0 rapidly goes toward 1, which means that A becomes quite large: the average chain length \bar{l} becomes too long to be correctly estimated by our analysis.

(c) **Chain Lengths Deduced from Diffuse Scattering Experiments.** In theory one could get a good deal of information from the study of diffuse sheets. In particular, in the induction period where polymer chains are well separated from one another, the diffuse intensity can be put into the form

$$I_D(\vec{k}) \propto x_p |F_p(\vec{k}) - F_m(\vec{k})|^2 \sum_N P(N) \frac{\sin^2(k_{\parallel} N b / 2)}{\sin^2(k_{\parallel} b / 2)} \quad (4)$$

where k_{\parallel} is the wave vector component in the chain direction. $P(N)$ represents the normalized chain length distribution function; i.e., $P(N)$ is the number of chains having N units divided by the total number of chains. Adapting a procedure described in ref 17, it could be possible to get $P(N)$ from a precise study of the

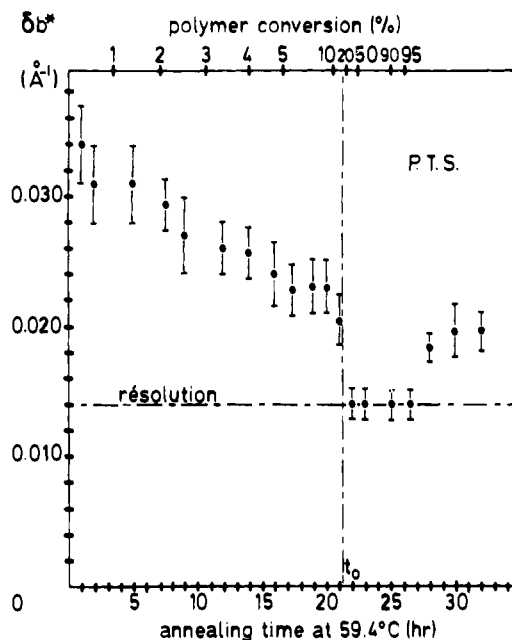


Figure 7. Experimental half-width at half-maximum (hwhm), δb^* , of diffuse sheets as a function of the annealing time at $59.4 \text{ }^\circ\text{C}$. The experimental resolution and the beginning of the autocatalytic period (t_0) are also indicated in the figure.

profile of $I_D(\vec{k})$ in the chain direction. The strong modulation of the diffuse intensity within each diffuse sheet can be explained by the factor $|F_p - F_m|$, which is the difference of structure factors of the polymer and monomer units, respectively. The prefactor x_p (polymer content) accounts for the weakness of the scattering. Owing to this weakness it has not been possible to extract such precise information from the study of the profile of diffuse sheets. We have been able to measure accurately only half the width at half-maximum (hwhm) of these sheets: δb^* . This quantity is given as a function of the annealing time (Figure 7). The first detected diffuse sheets (annealing time: 1 h; conversion: 0.25%) have a hwhm of 0.034 \AA^{-1} . The hwhm then regularly decreases in the induction part and rapidly drops to a limit value of 0.014 \AA^{-1} in the autocatalytic part, which corresponds to the experimental resolution. After an annealing time of 27 h (conversion: 97%), i.e., when the reaction is practically completed, δb^* slightly increases again. After 35-h annealing (conversion: >99%), the diffuse sheets cannot be observed anymore, even with longer exposure times.

Let us first assume that all polymer chains have nearly the same length $\bar{N}b$. This assumption will be discussed in section IV. So $P(N) \approx \delta(N - \bar{N})$ and we get from eq 4

$$I_D(\vec{k}) \propto x_p |F_p(\vec{k}) - F_m(\vec{k})|^2 \frac{\sin^2(k_{\parallel} \bar{N} b / 2)}{\sin^2(k_{\parallel} b / 2)} \quad (5)$$

The hwhm of such a diffuse intensity $\Delta k_{\parallel}^{1/2}$ is related to \bar{N} by the Scherrer formula:

$$\Delta k_{\parallel}^{1/2} = 0.888\pi / \bar{N}b \quad (6)$$

$\Delta k_{\parallel}^{1/2}$ can be obtained from the experimental value δb^* after correction of the experimental resolution δb_{res}^* . In such a case, it is better to use a Gaussian-type correction:¹⁵

$$\Delta k_{\parallel}^{1/2} = (\delta b^{*2} - \delta b_{\text{res}}^{*2})^{1/2} \quad (7)$$

Inserting this quantity into eq 6, we get the average chain length $\bar{l} = \bar{N}b$. Its variation as a function of x_p is given in Figure 8. The first chains have an average length $\bar{l} \approx 100 \text{ \AA}$ corresponding to $\bar{N} = 20$ units. This is in good agreement with the independent determination done in section III-b and with previous indirect

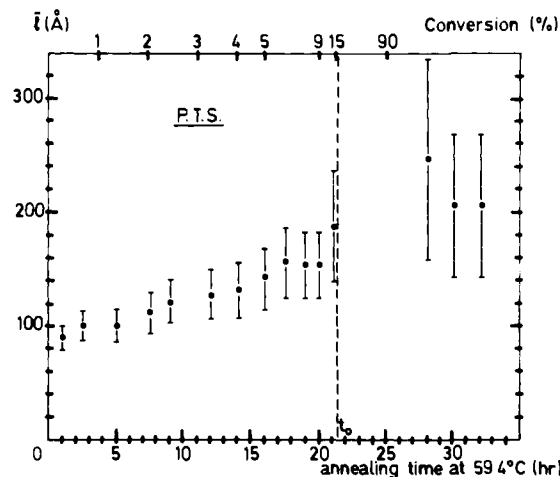


Figure 8. Average polymer length in the induction period and average monomer length at the end of the reaction deduced from X-ray diffuse scattering analysis. The left scale is in angstroms and the right one in b units. Below: annealing time at 59.4 °C. Above: polymer content.

determinations.⁸ As the reaction proceeds, \bar{l} regularly but slightly increases and reaches 200 Å ($N = 40$ units) after 21-h annealing, that is, just before the autocatalytic period. At the beginning of the autocatalytic period, the hwhm rapidly drops to the experimental resolution. It means that the average polymer chain length abruptly increases and becomes too long to be measured with our experimental setup. Assuming that we are able to detect a broadening of the sheets at the limit of error bars given in Figure 5, one obtains a lower limit of 400 Å. This limit can even be raised to 700 Å using data obtained at LURE. As already quoted, Mondong et al. observe by electronic microscopy polymer chains of about 5 μm in the autocatalytic period.⁹ These results will be discussed later. At the end of the reaction, for $x_p \geq 97\%$, Figure 7 shows that diffuse sheets become again broader than the resolution. In fact, we get a situation symmetric to that of the induction period: short monomer chains are embedded in a polymer matrix. Using expressions 6 and 7, we can estimate a monomer length of around 200 Å, that is, 40 units. This length does not appear to change strongly with the annealing time. This result can be understood in the following way: as monomer chains are in very suitable conditions for polymerization, they disappear suddenly one after one and do not shorten slowly with the annealing time.

IV. Spectroscopic Study of the Polymerization Mechanism of PTS

We have already stressed our lack of information about the real distribution function $P(N)$. In order to shed some light on this point, we have performed a study of the transmission spectrum of PTS crystals as a function of their polymerization degree. As already pointed out,¹⁸ the transmission spectrum may be readily interpreted as being due to polymer chains alone.

(a) Experimental Results. Figure 9 represents the observed spectra. The in situ polymerization has been performed at 75 °C and the annealing time is given on the right side of the figure. It is difficult to know precisely the beginning of the autocatalytic period because of lack of accuracy in the determination of the annealing temperature. First we observe the growth of a band system peaked at 572 nm. The position of the main peak does not vary markedly until 139 min ($x_p \approx 3\%$). Then it begins to red shift and broadens. After 243 min ($x_p \approx 9\%$) the peak is very large and its estimated position is 577 nm. At 255 min corresponding approximately to the beginning of the autocatalytic period, a second peak appears between 600 and 610 nm. Figure 9 shows more clearly the two peaks after 279 min of annealing time. The first peak disappears after 292 min of annealing and the second one regularly red shifts until 333 min where it locks at 618 nm, the value already found in the pure polymer.¹⁸ Figure

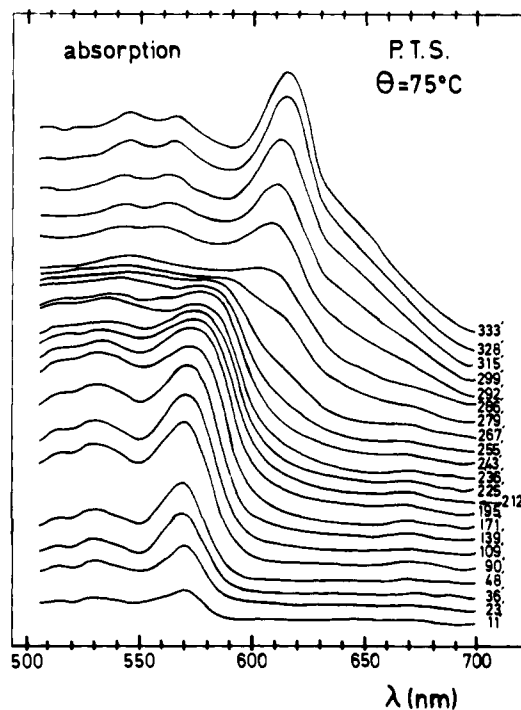


Figure 9. Absorption (in relative units) of PTS between 500 and 700 nm as a function of the annealing time at 75 °C. Spectra are composed of main peaks, the position of which is shown in Figure 10, and of secondary maxima at lower wavelengths corresponding to the vibrational structure of the polymer backbone.

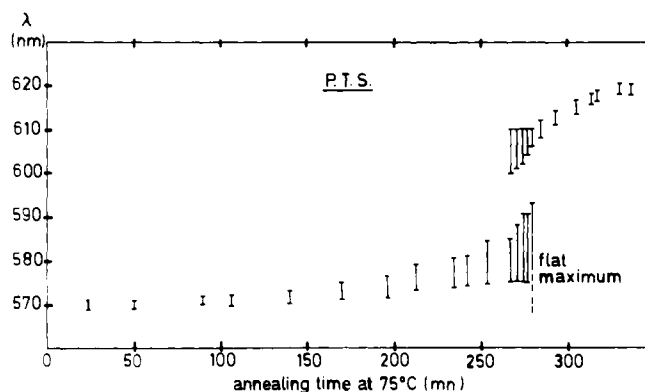


Figure 10. Wavelength of main peaks of spectra shown in Figure 9 as a function of the annealing time at 75 °C.

10 shows the position of the peaks as a function of the annealing time.

This experiment had previously been performed by Bloor et al.¹⁴ However, unlike this study, they report a continuous shift of the main peak from 572 to 618 nm. We have no explanation for this difference. With our conditions, the useful area of the plate was small enough to exclude any temperature gradient on it, and crystals were of correct quality and about the same size as those used by Bloor et al. Moreover, the experiment has been repeated twice at 75 °C and once at 80 °C with always the same result. In the following, we shall discuss our results in connection with the X-ray diffuse scattering chain length determination.

(b) Discussion. The main point to understand is the shift of the main peak in the induction period and the appearance of a second maximum at the beginning of the autocatalytic period.

The maximum of absorption in PTS is believed to correspond to an excitonic transition.¹⁹ Two factors can act to change the energy of such a transition: the strain experienced by the polymer chains increases its energy,²⁰ the length of the polymer chains,

(18) Bloor, D.; Preston, F. H. *Phys. Status Solidi A* 1976, 37, 427.

(19) Philpott, M. R. *Chem. Phys. Lett.* 1977, 50, 18.

(20) Batchelder, D. N.; Bloor, D. *J. Phys. C* 1978, 11, L629.

when increasing, decreases its energy.²¹ The difficulty is that these two factors are present at the same time, and their respective contributions can barely be separated. In connection with X-ray diffuse scattering results obtained in section III, we could present the following explanation of the behavior of the spectrum:

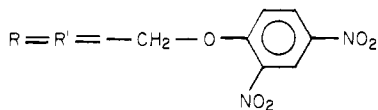
(1) First short chains (~ 100 Å) account for the peak centered at 572 nm. This value must be due both to the shortness of chains and to their traction. Furthermore, experiments performed at low temperature²² have shown that the peak is quite narrow. Thus, the distribution function is well peaked on the average chain length, and the use of the function $P(N) \approx \delta(N - \bar{N})$ at the beginning of the reaction can be justified.

(2) As the reaction proceeds, the relaxation of the stress exercised by the monomer matrix upon the chains has two consequences: first a red shift of the spectrum of the already formed chains and secondly the new-formed chains are slightly longer as shown by X-ray diffraction results. Thus, the distribution function $P(N)$ broadens toward longer chains explaining the shift and the broadening of the main peak toward longer wavelengths. So when $x_p \geq 3\%$, the use of $P(N) \approx \delta(N - \bar{N})$ and consequently of formulas 6 and 7 can be less justified than at the very beginning of the reaction.

At the beginning of the autocatalytic period, very long chains appear, creating the second peak observed at higher wavelengths. The disappearance of the first peak can be due either to the fact that it is buried under the second peak or to the rapid disappearance of the short chains. The further shift of the second peak comes from the final relaxation of the matrix stress.

V. Conclusion

The main result of this paper is that independent X-ray and spectroscopic measurements give a somewhat unified picture of the topochemical polymerization mechanism of PTS. A similar picture will be given in a forthcoming paper on another diacetylenic compound: 1,6-bis(2,4-dinitrophenoxy)-2,4-hexadiyne (abbreviated as DNP) where²³



In PTS, the thermal polymerization proceeds homogeneously: polymer chains grow at random in the monomer matrix with a

common parameter b throughout the reaction. In the induction period, that is, for $x_p \leq 15\%$, polymer conversion increases by the formation of short polymer chains which are in extension with respect to their periodicity in the pure polymer. First chains are around 100 Å long (20 units) with a distribution function well peaked on the average value. As x_p increases, the lattice parameter b slightly decreases and the growth of somewhat longer chains is favored. As a consequence the distribution function $P(N)$ broadens toward longer chain lengths. At the end of the induction period, the average chain length is about 200 Å long (40 units). We have no clear explanation for the exact mechanism that limits the growth of a chain to the above quoted values. In the autocatalytic period, polymer chains suddenly become longer by at least 2 orders of magnitude (around $5 \mu\text{m}^9$). After this period, a few percent of monomer remains under the form of short monomer chains that slowly disappear.

It has been reported elsewhere²⁵ that pure monomer of PTS presents an incommensurate modulated phase between 206 and 163 K. Below 163 K, there is a lock-in transition to a $2a \times b \times c$ superstructure. This structural phase transition seems to involve mainly side groups R. However, although the polymerization reaction modifies mainly the four central carbons arrangement, it has been found²⁵ that the degree of polymerization had a strong influence on the phase diagram of PTS. In particular the lock-in temperature shows a large decrease (of about 10 K) when the studied crystal is slightly annealed. On the other side the upper transition temperature (206 K) does not change markedly. This result shows that the first polymer chains have an unexpected stabilization effect on the incommensurate phase, in spite of the perturbation brought by these chains in the modulation. Although we have not a detailed explanation for this phenomenon, it is quite interesting to remark that the average length of first chains, $20b$, compares well with the wavelength $(1/\delta)b$ (with $\delta \leq 0.06$) of the incommensurate modulation which occurs in the same direction. The coincidence of the periodicity of the modulation with the length of the first polymer chains might be at the origin of the stabilization of the incommensurate phase toward lower temperatures.

Acknowledgment. We are very grateful to M. Bertault for the use of its conversion curve of PTS. We acknowledge also useful discussions with R. Comès and M. Schott and the technical help of S. Megtert for the preliminary experiment performed at station D 16 of LURE.

Registry No. PTS, 32527-15-4.

(21) Exarhos, G. J.; Risen, W. M.; Baughmann, R. H. *J. Am. Chem. Soc.* **1976**, *98*, 481.

(22) Bloor, D.; Hubble, G. L. *Chem. Phys. Lett.* **1978**, *56*, 89.

(23) Albouy, P. A.; Pouget, J. P., to be submitted for publication.

(24) Robln, P.; Pouget, J. P.; Comès, R.; Moradpour, A. *Chem. Phys. Lett.* **1980**, *71*, 217.

(25) Patllon, J. N.; Robin, P.; Albouy, P. A.; Pouget, J. P.; Comès, R. *Mol. Cryst. Liq. Cryst.* **1981**, *76*, 297.